

## Small-angle and wide-angle X-ray scattering study on the bilayer structure of synthetic and bovine heart cardiolipins

This article has been downloaded from IOPscience. Please scroll down to see the full text article.

2010 J. Phys.: Conf. Ser. 247 012021

(<http://iopscience.iop.org/1742-6596/247/1/012021>)

View [the table of contents for this issue](#), or go to the [journal homepage](#) for more

Download details:

IP Address: 134.160.214.29

The article was downloaded on 11/10/2011 at 02:37

Please note that [terms and conditions apply](#).

## Small-angle and wide-angle X-ray scattering study on the bilayer structure of synthetic and bovine heart cardiolipins

Hiroshi Takahashi<sup>1,3,4</sup>, Tomohiro Hayakawa<sup>2,3</sup>, Kazuki Ito<sup>4</sup>, Masaki Takata<sup>4</sup>,  
Toshihide Kobayashi<sup>3</sup>

<sup>1</sup> Biophysics Laboratory, Department of Chemistry and Chemical Biology, Gunma University, Maebashi, Gunma, 371-8510, Japan

<sup>2</sup> Life Science Laboratory, Advanced Materials Laboratories, Sony Corporation, Yushima, Bunkyo-ku, Tokyo, 113-8510, Japan

<sup>3</sup> Lipid Biology Laboratory, RIKEN, Wako, Saitama 351-0198, Japan

<sup>4</sup> Structural Materials Science Laboratory, RIKEN SPring-8 Center, Sayo, Hyogo 679-5148, Japan

E-mail: htakahas@chem-bio.gunma-u.ac.jp

**Abstract.** Cardiolipin (CL) is a membrane phospholipid containing four fatty acid chains. CL plays an important role in energy transformation in mitochondria. The disorder of CL biosynthesis is involved in a genetic disease, Barth syndrome. Alteration of fatty acid composition of CLs has been found in Barth syndrome patients, i.e., the decrease of unsaturated fatty acid chains. In this study, we investigated how the degree of saturation alters the structure of CL bilayers by using X-ray scattering. Bovine heart CL and two synthetic CLs were compared. Fatty acid compositions of these three CLs have different saturation. Small-angle X-ray scattering data showed that the decrease of the number of double bonds in the unsaturated fatty acid chains causes to thicken the CL bilayers. In addition, wide-angle X-ray scattering data suggested that the decrease reduces the degree of disorder of the hydrophobic region in a liquid crystalline phase. These results may be related to the dysfunction of mitochondria in Barth syndrome.

### 1. Introduction

Cardiolipin (CL) is a unique membrane lipid [1]. It is a phospholipid dimer that contains four fatty acids. Two phosphatidyl groups are esterified to a single glycerol. CL was first isolated from heart [2] and is almost exclusively located in the inner membrane of mitochondria, where it represents the 25-30% of total mass [3]. The function of mitochondria is creation of adenosine triphosphate (ATP) used as a common chemical energy molecule for living things. It is well-known that CL is required for the ATP production [1,4]. The ATP synthesis is associated with several protein complexes embedded in the inner mitochondrial membrane, so-called mitochondrial respiratory chain complexes (I - IV). Biochemical and biophysical studies have revealed that CL is needed to stabilize the native structure of the complexes III and IV [5,6].

There are several diseases related to the dysfunction of mitochondria. One of such example is Barth syndrome [7]. The syndrome patients suffer from delayed growth, weakness of heart muscle,

and disorder of immune system. Barth syndrome is an X-linked disease associated with mutations in the *tafazzin* gene that codes an enzyme involved in CL synthesis [8]. In fact, recent biochemical studies have revealed that Barth syndrome induces the change of fatty acid composition of CL [9,10]. Normal heart CL contains mainly 18:2 unsaturated fatty acid (linoleic acid) chains. By contrast, in CLs of Barth syndrome patients, various fatty acid chains are found and the amount of saturated fatty acid chains increases particularly [9,10]. Thus, the disorder of CL synthesis seems to be a cause of the mitochondrial dysfunction observed in Barth syndrome. The molecular mechanism of the disease, however, remains unknown yet.

Theoretical and experimental studies have indicated that the physical properties of phospholipid bilayers affect the membrane protein functions [11,12]. In transmembrane protein-lipid interaction, one important factor is a matching of hydrophobic part lengths between the proteins and lipid bilayers. If the hydrophobic part lengths differ each other under non-stress conditions, this mismatch does not induce the hydrophobic parts of either lipid or protein to expose water but induces conformational change of either protein or lipid or both to compensate the mismatch. The conformational change of protein affects its activity. In other words, the thickness of lipid bilayer parts of biomembranes affects transmembrane protein's activity [12,13]. This concept has been supported by several studies using a model system where an ion pump protein is incorporated into a model membrane made from a single phospholipid species. Such studies have revealed that the activity of ion pump depends on the number of carbon atoms in the fatty acid chains of phospholipid [14,15].

The final goal of our study is to clarify the molecular mechanism how the disorder of CL synthesis causes the mitochondrial dysfunction in Barth syndrome. As the first step, in this study, we investigated how the degree of saturation of the hydrocarbon chain alters the structure of CL bilayers by using X-ray scattering. We used three different CLs, i.e., natural bovine heart CL (Heart CL), synthetic tetraoleoyl-CL (TOCL) and synthetic tetramyristoyl-CL (TMCL). The principal fatty acid component of the heart CL is linoleic acid having two *cis* double bonds [9,10]. TOCL is a mono-unsaturated CL and TMCL is a saturated CL. The latter two CLs were chosen as CLs found in Barth syndrome patient contain saturated and monounsaturated fatty acids.

## 2. Experimental

### 2.1. Materials

All lipid powder samples used in this study, natural cardiolipin extracted from bovine heart tissue (Heart CL), synthetic 1',3'-bis[1,2-dioleoyl-*sn*-glycero-3-phospho]-*sn*-glycerol (tetraoleoyl-cardiolipin, TOCL) and 1',3'-bis[1,2-dimyristoyl-*sn*-glycero-3-phospho]-*sn*-glycerol (tetramyristoyl-cardiolipin, TMCL) were purchased from Avanti Polar Lipids, Inc. (Alabaster, AL). All lipids were used without further purification.

### 2.2. X-ray scattering measurements

Lipid film was formed from a chloroform solution of lipids under a stream of nitrogen gas, dried in high vacuum overnight, and then hydrated and vortexed with buffers. The buffer solution (pH 7.4) was 20 mM 4-(2-hydroxyethyl)-1-piperazineethanesulfonic acid (HEPES) buffer with 100 mM NaCl and 10 mM ethylenediaminetetraacetic acid (EDTA). Because it has been reported that the phase behaviour of CL is sensitive to the presence of Ca<sup>2+</sup> ions [16], EDTA was added to the buffer to remove free Ca<sup>2+</sup> ions. The lipid concentration of the samples was 50 mM. This corresponds to about 1,000 water molecules per a lipid. To the best of our knowledge, there is no paper reporting the numbers of bound water or interlamellar water molecules for CLs. Judging from the literature data of other phospholipids, for example, about 30 waters per an egg phosphatidylcholine [17], it can be assumed that 50 mM CL solution contains excess water. After mixing about 5 minutes by vortex mixer at room temperature, the sample solutions were visually clear and homogenous.

X-ray scattering measurements were carried out at RIKEN Structural Biology Beamline I (BL45XU) at SPring-8. The optical system of the beamline has been described elsewhere

[18]. X-ray scattering data were collected with a RAXIS-IV imaging-plate area detector (Rigaku). The sample-to-detector distance was about 550 mm. The digital two-dimensional intensity data were transformed into one-dimensional intensity data as a function of  $q = 4\pi\sin\theta/\lambda$ , where  $2\theta$  is the scattering angle and  $\lambda$  is the wavelength of X-ray (0.090 nm), by circular averaging using a FIT2D software developed by Dr. A. Hammersley (<http://www.esrf.fr/computing/scientific/FIT2D/>). The scattering angle ( $2\theta$ ) was calibrated with silver behenate powder crystals [19]. Samples were measured in a sample cell with a path length of 1.5 mm and a pair of thin quartz windows (thickness of 20  $\mu\text{m}$  each).

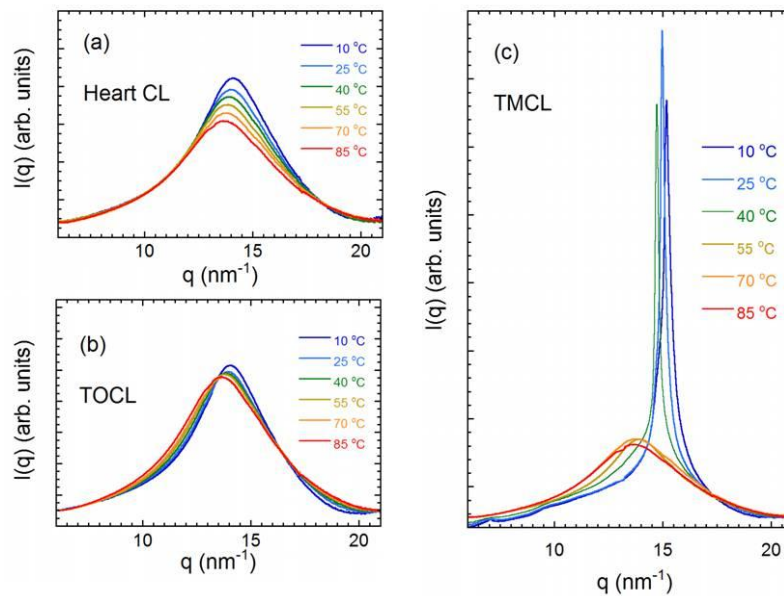


**Figure 1.** Temperature dependence of wide-angle X-ray scattering profiles for (a) Heart CL, (b) TOCL, and (c) TMCL.

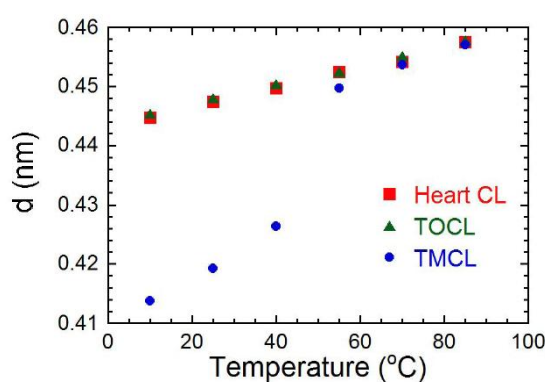


**Figure 2.** Wide-angle spacings ( $d$ ) plotted versus temperature. (■) Heart CL, (▲) TOCL, and (●) TMCL.

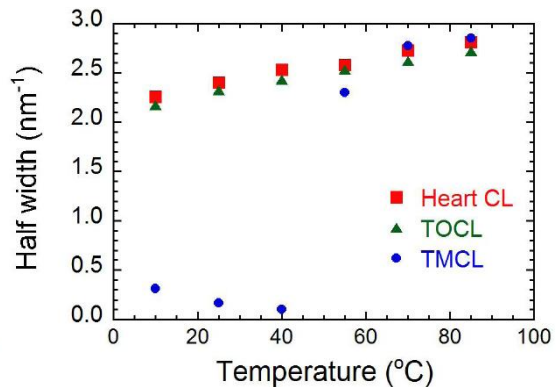


**Figure 3.** Half width at half maximum of the wide-angle bands plotted versus temperature. (■) Heart CL, (▲) TOCL, and (●) TMCL.

Sample solutions were transferred to the sample cell by syringe through the hole with the diameter of 1 mm of the cell. It is known that dehydration affects the phase behaviour of CLs [20]. To prevent evaporation of water through the hole during measurements (the samples were heated up to 85 °C), the hole was tightly covered by using Parafilm®. The scattering data were not used when any volume changes of the sample solution or any bubbles were detected by visual inspection after measurements. The sample cell was attached to a sample folder. The cell was in good thermal contact with the folder whose temperature was controlled to  $\pm 0.01$  °C with a high-precision thermoelectric device. The exposure time was 60 sec.

### 3. Results

#### 3.1. Wide-angle X-ray scattering

Figure 1 shows X-ray scattering profiles of the wide-angle region for three different CLs, Heart CL, TOCL, and TMCL. The scattering from the hydrocarbon chain packing appears in this region. Figure 2 presents the  $d$ -spacings calculated from the maximum positions. Figure 3 displays the values of half width at half-maximum determined by fitting Lorentz shape function with linear background.

Except for TMCL at low temperatures (below 40 °C, Fig. 1(c)), only broad band centred at about  $q = 14 \text{ nm}^{-1}$  ( $d = 0.45 \text{ nm}$ ) was observed, indicating that the hydrocarbon chains are melted, i.e., they are in a liquid crystalline phase. The sharp peaks observed for TMCL showed that TMCL is in a gel phase at low temperatures. By using differential scanning calorimetry, the transition temperature was measured for TMCL dispersed into the same HEPES buffer used in the present X-ray study (data not shown). The temperature was 41.5 °C, agreeing with the disappearance of the sharp diffraction peak above 40 °C.

Both  $d$ -spacings and the values of half width increased with rising of temperature for all three CLs in the liquid crystalline phase. This indicates that the increasing temperature induces conformational disorder of the hydrocarbon chains. At the same temperature, the  $d$ -spacings of TMCL in the liquid crystalline phase are almost the same as those of other CLs, however, the half width of Heart CL was slightly wider than that of TOCL. The latter result suggests that the increase of number of *cis* double bonds decreases the structural regularity in the melted chains.

#### 3.2. Small-angle X-ray scattering

Small-angle X-ray scattering profiles obtained at different temperatures are shown in Fig. 4. In the figure,  $q^2 I(q)$  is plotted as a function of  $q$ , where  $I(q)$  is one-dimensional intensity data transformed from two-dimensional data recorded on imaging plate by circular averaging, i.e. it corresponds to the data obtained by using a one-dimensional detector, and  $q^2$  corresponds to the Lorentz-polarization (LP) factor for unoriented samples. Therefore,  $q^2 I(q)$  is proportional to the square of the Fourier transform of one-dimensional electron density profile of the sample, i.e., form factor [21,22].

In the electron density profiles of phospholipid bilayers, the polar head group regions have the highest values. Based upon model calculations, Engelman [23] have shown that, if the highest peak-to-peak distance is kept constant, the modulation of model electron density affects mainly the shape of the first band of the form factor, however, hardly affects the peak position of second band. Hence, the position of second maximum in the  $q^2 I(q)$  curve is a good measure of the average bilayer thickness. Figure 5 represents the bilayer thickness values estimated by this method. For the liquid crystalline phase, the decreases of bilayer thickness ( $D_B$ ) were not linear but exponential. Table 1 shows the parameters estimated by fitting the bilayer thickness with an equation of  $D_B = D_0 \exp(E/k_B T)$ , where  $D_0$  and  $E$  are parameters,  $k_B$  is the Boltzmann constant, and  $T$  is absolute temperature. Although the carbon number of the chains is the same 18, the bilayer thickness of Heart CL is thinner than that of TOCL. This indicates that the existence of *cis* double bond in the hydrocarbon chains greatly reduces the bilayer thickness.

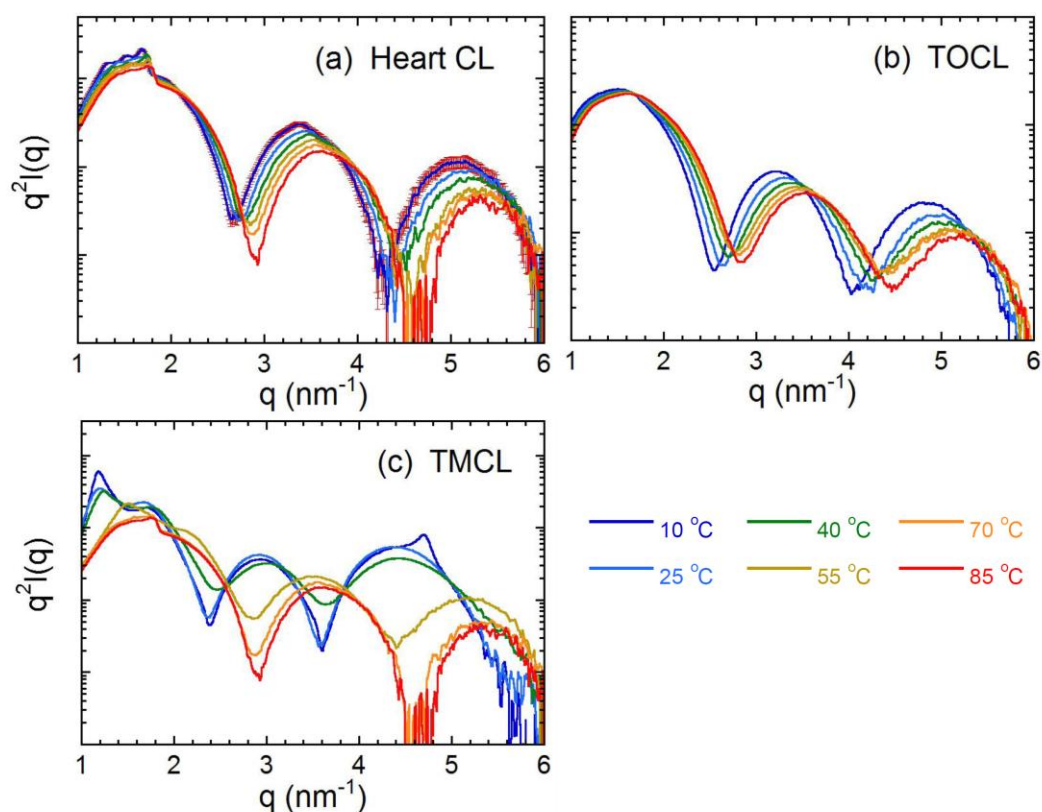


**Figure 4.** Temperature dependence of corrected small-angle X-ray scattering intensity curves ( $q^2 I(q)$ ) for (a) Heart CL, (b) TOCL, and (c) TMCL. Error bars (the square root of counts) are shown for the curve of Heart CL at 10°C. Because the other curves have almost the same error values, these error bars are omitted for clarity.

For TMCL at 10 °C, two diffraction peaks were observed at  $q = 1.176 \text{ nm}^{-1}$  and  $4.703 \text{ nm}^{-1}$ . These are the first and fourth lamellar diffraction peaks, respectively, corresponding to the lamellar spacing of 5.38 nm. This value is fairly close to that reported for TMCL dispersed into sodium phosphate buffer at 2 °C (5.42 nm) [24]. Above 25 °C, the fourth peak disappeared and the lamellar spacing shifted toward to shorter direction with increasing temperature ( $D = 5.34 \text{ nm}$  at 25 °C,  $D = 5.13 \text{ nm}$  at 40 °C).

For Heart CL, some broad diffraction peaks with asymmetric shape appeared in the range of  $q = 1.2$  to  $1.8 \text{ nm}^{-1}$ . Although the peak positions were not reproducible perfectly, the broad peaks in this region appeared in all our experiments (see Appendix). At present, the assignment of these diffraction peaks remains unresolved.

#### 4. Discussion

From biological viewpoints, the most important result of this study is that the bilayer thickness of Heart CL is thinner than that of TOCL. In other words, the reduction of the number of double bonds induces to thicken the cardiolipin membranes. It has been pointed out that bilayer thickness has a large effect on the activities of many membrane proteins [12-15]. i.e., there is an optimal thickness for protein's activity. In the CLs extracted from normal heart muscle, the main components are tetralinoleoyl-CL containing four linoleic acid (18:2), and trilinoleoyl-oleoyl-CL containing three linoleic acid (18:2) and one oleic acid (18:1) [9]. On the other hand, in the CLs extracted from the

heart muscle of Barth syndrome patients, dominant components are CLs containing palmitic acid (16:0), stearic acid (18:0), oleic acid (18:1), and so on. [9,10]. Based upon these data and the result of this study, it is likely that the thickness of inner mitochondrial membrane of Barth syndrome patients is thicker than that of normal. This would be the origin for dysfunction of membrane protein(s) in mitochondria in Barth syndrome.

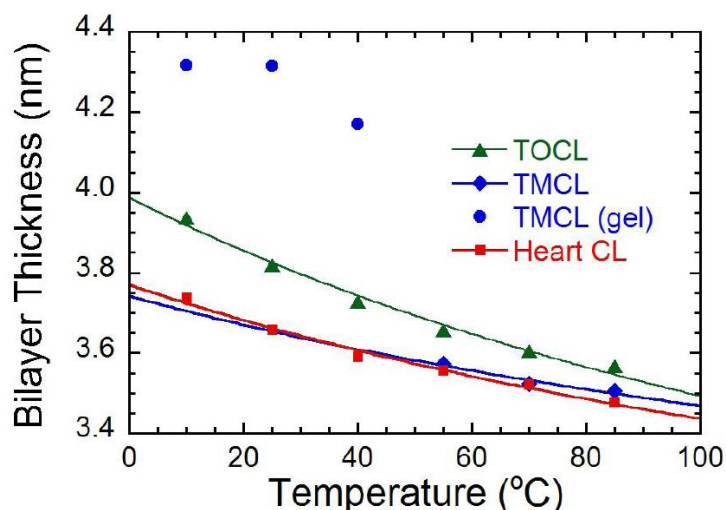


**Figure 5.** Estimated values of bilayer thickness from maximum positions of the second band of  $q^2I(q)$  curves plotted versus temperature. (■) Heart CL, (▲) TOCL, and (●) TMCL.

**Table 1. Fitting parameters of the bilayer thickness (see text)**

	Heart CL	TOCL	TMCL
$D_0$ (nm)	2.67	2.43	2.82
$E$ (J)	$6.84 \times 10^{-22}$	$9.77 \times 10^{-22}$	$5.60 \times 10^{-22}$

In this study, the bilayer thickness was estimated according to a simple method proposed by Engelman [23]. Here we discuss the reliability of this method. Recently, Lewis *et al.* [24] reported the phase behaviour and structure of TMCL. In their study, the electron density profiles of TMCL bilayers were reconstructed from X-ray diffraction data of the multilamellar vesicles by using Caillé [25] and paracrystalline [26] theories for disorder of the lamellar stacking. From the reconstructed electron density profiles, the phosphate-phosphate distances across the bilayer ( $d_{pp}$ ) were estimated to be 4.35 nm at 35 °C and 3.78 nm at 55 °C, respectively [24]. Our bilayer thickness values (4.17 nm at 40 °C, 3.57 nm at 55 °C) are slightly thinner than those of Lewis *et al.*, but the difference before and after the melting transition is in good agreement with each other (about 0.6 nm). Hence, the bilayer thickness estimation method used here is reliable for the relative comparison. However, careful treatments should be needed for the estimation of absolute values.

At room temperature, the difference of estimated bilayer thickness between TOCL and Heart CL was about 0.2 nm. The similar value has been reported for the difference between dioleoyl-phosphatidylcholine and dilinoleoyl-phosphatidylcholine [27]. Lewis and Engelman [28] found a linear increase of bilayer thickness with the number of carbon of acyl chain for saturated and monounsaturated phosphatidylcholines. The degree of increase was 0.175 nm per carbon atom. If the

same increase is assumed for CLs, the bilayer thickness of CL having four 16-carbon saturated fatty acid (palmitic acid) chains that appears in Barth syndrome patients, is about 0.3 nm thicker than Heart CL based on the results of TMCL. As shown by the width of scattering band in wide-angle region, the two *cis* double bonds in one hydrocarbon chain introduce more randomness in the hydrophobic core in the bilayers by comparison with only one double bond. The randomness leads expansion of the occupied area per lipid [29]. Thereby, the reduction of bilayer thickness takes place, although the same numbers of carbon atoms are contained in the chains.

Lewis *et al.* [24] studied the effects of different buffer solution on TMCL's polymorphic phase behaviour. They have reported that the melting transition temperatures for TMCL dispersed into Tris and phosphate buffers are 38.9 °C and 41.2 °C, respectively. They have also shown the existence of a subgel phase with an orthorhombic subcell that transforms into the gel phase at about 25 °C on heating. In this study, HEPES buffer was used and the melting transition temperature was 41.5 °C. A broad peak was detected at around 28 °C in our differential scanning calorimetric measurements (data not shown). This peak may correspond to a subgel-to-gel phase transition. However, an orthorhombic subcell was not clearly observed in the present X-ray study. The peak shape of TMCL at 10 °C was slightly asymmetric, i.e., a small broad shoulder peak appeared at the small-angle side. In addition, the half width of the TMCL's sharp diffraction peak at low temperatures decreased with increasing temperature (Fig.3). These results might be related to the formation of the subgel phase. However the subgel phase is not a main issue of the present study and we leave it to future work.

Another problem that requires further detailed future study is the assignment of diffraction peaks appeared in the small-angle region of heart CL. The three peaks were asymmetric and have some shoulders. These peaks should be resolved into more than three by high resolution measurements.

Our study predicts that the mitochondrial membrane from Barth syndrome patients is thicker than that of normal subject. Future biophysical and cell biological analysis of CL in both model and biomembranes will clarify the molecular significance of CL in Barth syndrome.

#### Acknowledgements

This work was supported by Barth Syndrome Grant 2007-2008 from the Barth Syndrome Foundation and Lipid Dynamics Project of RIKEN. The synchrotron radiation experiments were performed at BL45XU in SPring-8 with the approval of RIKEN (Proposal No. 20080023 and 20090067).

- [1] Haines T H 2009 *Biochim. Biophys. Acta* **1788** 1997
- [2] Pangborn M C 1947 *J. Biol. Chem.* **168** 351
- [3] Hostetler K Y and van Den Bosch H 1972 *Biochim. Biophys. Acta* **260** 380
- [4] Robinson N C, Zborowski J and Talbert L H 1990 *Biochemistry* **29** 8962
- [5] Zhang M, Mileykovskaya, E and Dowhan W 2002 *J. Biol. Chem.* **277** 43553
- [6] Pfeiffer K, Gohil V, Stuart R A, Hunte C, Brandt U, Greeberg M L and Schägger H 2003 *J. Biol. Chem.* **278** 52873
- [7] Barth P G, Scholte H R, Berden J A, van der Klei-van Moorsel JM, Luyt-Howen I E M, van't Veer-Korthof E T, van der Harten J J and Sobotka-Plojhar M A 1983 *J. Neurol. Sci.* **62** 327
- [8] Schlame M and Ren M 2006 *FEBS Lett.* **580** 5450
- [9] Schlame M, Towbin J A, Heerdt P M, Jehle R, DiMauro S, Blanck T J J 2002 *Ann. Neurol.* **51** 634
- [10] Schlame M, Ren M, Xu Y, Greenberg M L and Haller I 2005 *Chem. Phys. Lipids* **138** 38
- [11] Mouritsen O G 2005 *Life as a Matter of Fat: The Emerging Science of Lipidomics* (Berlin: Springer)
- [12] Heimburg T 2007 *Thermal Biophysics of Membranes* (Weinheim: Wiley-VCH)
- [13] Mouritsen O G and Bloom M 1984 *Biophys. J.* **46** 141



- [14] Lee A G 1998 *Biochim. Biophys. Acta* **1376** 381
- [15] Cornelius F 2001 *Biochemistry* **40** 8842
- [16] Rand R P, Sengupta S 1972 *Biochim. Biophys. Acta* **255** 484
- [17] Nagle J F, Tristram-Nagle S, 2000 *Biochim. Biophys. Acta* **1469** 159
- [18] Fujisawa T, Inoue K, Oka T, Iwamoto H, Uruga T, Kumasaka T, Inoko Y, Yagi N, Yamamoto M and Ueki T 2000 *J. Appl. Cryst.* **33** 797
- [19] Huang T C, Toraya H, Blanton T N and Wu Y 1993 *J. Appl. Cryst.* **26** 180
- [20] Alessandrini A, Muscatello U 2009 *J. Phys. Chem. B* **113** 3437
- [21] Glatter O and Kratky O 1982 *Small Angle X-ray Scattering* (New York: Academic Press)
- [22] Takahashi H and Ito K 2007 *J. Phys. Conference Ser.* **83** 012022
- [23] Engelman D M 1971 *J. Mol. Biol.* **58** 153
- [24] Lewis R N A H, Zwegyick D, Pabst G, Lohner K and McElhaney R N 2007 *Biophys. J.* **92** 3166
- [25] Zhang RT, Suter R M and Nagle J F 1994 *Phys. Rev. E.* **50** 5047
- [26] Guinier A 1963 *X-ray diffraction in crystals, imperfect crystals, and amorphous bodies* (San Francisco : W. H. Freeman)
- [27] Rawick W, Olbrich K C, McIntosh T, Needham D and Evans E 2000 *Biophys. J.* **79** 328
- [28] Lewis B A and Engelman D M 1983 *J. Mol. Biol.* **166** 211
- [29] Hub J S, Salditt T, Rheinstädter M C and de Groot B L 2007 *Biophys. J.* **93** 3156

## Appendix

Figure 6 represents small-angle X-ray scattering intensity curves of heart CL at 25 °C. The two different curves were obtained from two different samples prepared under the same condition. The arrows indicate the corresponding position of the beamstop edge. Except for the peak at  $q = 0.8 \text{ nm}^{-1}$  and broad peak(s) in  $q = 1.2$  to  $1.8 \text{ nm}^{-1}$ , the two curves are almost identical to each other. Judging from the position of the beamstop, the peak(s) in  $q = 1.2$  to  $1.8 \text{ nm}^{-1}$  would not be due to the scattering from the beamstop. At present, the origin of these peaks cannot be assigned; at least, the existence of these peaks does not affect the estimation of the bilayer thicknesses.

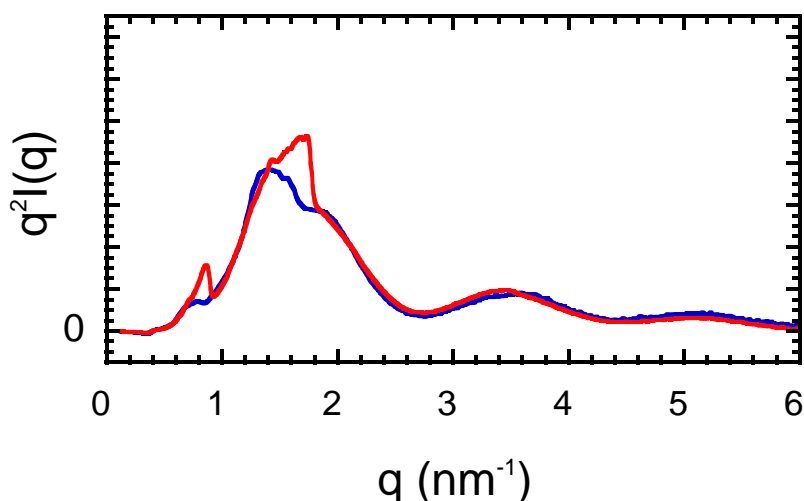


**Figure 6.** Reproducibility of small-angle X-ray scattering intensity curve of heart CL. These curves were recorded at 25 °C. The arrow indicates the position of the beamstop edge. Differing from Fig.4, the vertical axis is linear.